Ionic core–shell dendrimers with a polycationic core: structural aspects and host–guest binding properties†

Rob van de Coevering,[a] Pieter C. A. Bruijnincx,[a] Martin Lutz,[b] Anthony L. Spek,[b] Gerard van Koten*[a] and Robertus J. M. Klein Gebbink*[a]

Received (in Montpellier, France) 30th November 2006, Accepted 18th April 2007
First published as an Advance Article on the web 15th May 2007
DOI: 10.1039/b617669k

The structural aspects and host–guest binding properties of ionic core–shell dendrimers [**1**]Br_8 and [**2**]Br_4, which bear a polycationic core and a neutral shell of Fréchet-type poly(benzyl aryl ether) dendrons, have been investigated by means of dendritic wedges [**3**]Br_2 and [**4**]Br, that resemble one of the four wedges of the dendrimers. Alike the dendrimers, dendritic wedges [**3**]Br_2 and [**4**]Br form discrete stoichiometric assemblies with Methyl Orange anions to give host–guest assemblies [**3**][MO]$_2$ and [**4**][MO], respectively. X-Ray crystal structures of dendritic wedge [**3**]Br_2 and host–guest assembly [**4**][MO] have been resolved and reveal that besides Coulombic interactions additional interactions, such as weak hydrogen bonds and π–π interactions, can also be present between the dendritic host and substrate molecules. The substrate selectivity of the ionic core–shell dendrimers for sulfonato anions over carboxylato anions, as was observed in preliminary competition experiments, can be attributed to these additional binding interactions. These X-ray structures, furthermore, substantiate earlier speculations in literature on the presence of π–π interactions between Fréchet-type poly(benzyl aryl ether) dendritic wedges and aromatic substrate molecules.

Introduction

During the last two decades several research groups have investigated the possibility of using dendrimers as host molecules for (in)organic guest molecules.[1] In these dendritic host–guest complexes, substrate molecules are either physically entrapped in the voids of the dendritic structure[2] or bound to receptor units within the dendritic structure *via* non-covalent interactions, *e.g.* solvophobic interactions,[3] hydrogen bonds,[4] or Coulombic interactions.[5] These receptor units are located either in the interior (close to the core) of the dendritic structure (endo-receptor sites) or at the periphery of the dendrimer (exo-receptors).

Recently, our group has introduced a novel class of ionic core–shell dendrimers that carry a given number of cationic sites, *i.e.* quaternary ammonium groups at the core, which are decorated with a soft condensed shell of neutral Fréchet-type poly(benzyl aryl ether) dendrons (see dendrimers [**1**]Br_8 and [**2**]Br_4, Fig. 1).[6] A binding study carried out with the Methyl Orange anion (MO)[7] as guest molecule revealed that these polycationic dendrimers bind a stoichiometric number of these anionic MO guest molecules based on the number of quaternary ammonium sites in the core (Fig. 2). Apparently, the maximum number of accommodated guest molecules does not depend on the extent of steric crowding in the dendritic shell, as was demonstrated in binding studies with dendrimers up to the second generation. The non-covalent binding of MO by these dendrimers involves an ion exchange reaction between bromide anions and excess of the sodium salt of MO in a biphasic set-up of dichloromethane and water. The reversible character of Coulombic interactions allows for the controlled and quantitative release of MO guest molecules by applying to the dendrimer–MO assembly an external stimulus, *e.g.* an acid or an excess of a salt with a competitive anion.[6] Other applications of these ionic core–shell dendrimers were found in homogeneous catalysis. We have reported the use of the first generation octa-cationic dendrimer $[\mathbf{1}]^{8+}$ as a noncovalent support for catalytically active Pd(II) complexes.[8]

In order to gain more insight in the structural aspects and the host–guest binding properties of these ionic core–shell dendrimers, we have separately investigated the non-covalent binding interactions of molecular components that represent defined structural sections of the dendrimers. The X-ray crystal structures of dendritic wedge [**3**]Br_2 and host–guest assembly [**4**][MO] (Fig. 1 and 2), which resemble one of the four wedges of ionic core–shell dendrimers [**1**]Br_8 and dendrimer-MO assembly [**2**][MO]$_4$, respectively, are presented. The crystal structures of these model species substantiate that besides Coulombic interactions, additional binding interactions, such as hydrogen bonds and π–π interactions, could also contribute to the binding in host–guest assemblies formed between the ionic core–shell dendrimers and anionic substrate

[a] *Organic Chemistry and Catalysis, Faculty of Science, Utrecht University, Padualaan 8, 3584 CH Utrecht, The Netherlands. E-mail: g.vankoten@chem.uu.nl; r.j.m.kleingebbink@chem.uu.nl; Fax: (+31) 30 252 3615; Tel: (+31) 30 253 3210/1889*
[b] *Bijvoet Center for Biomolecular Research, Crystal and Structural Chemistry, Faculty of Science, Utrecht University, Padualaan 8, 3584 CH Utrecht, The Netherlands. E-mail: a.l.spek@chem.uu.nl; Fax: (+31) 30 253 3940; (+31) 30 253 2538*

† This paper was published as part of the special issue on Dendrimers and Dendritic Polymers: Design, Properties and Applications.

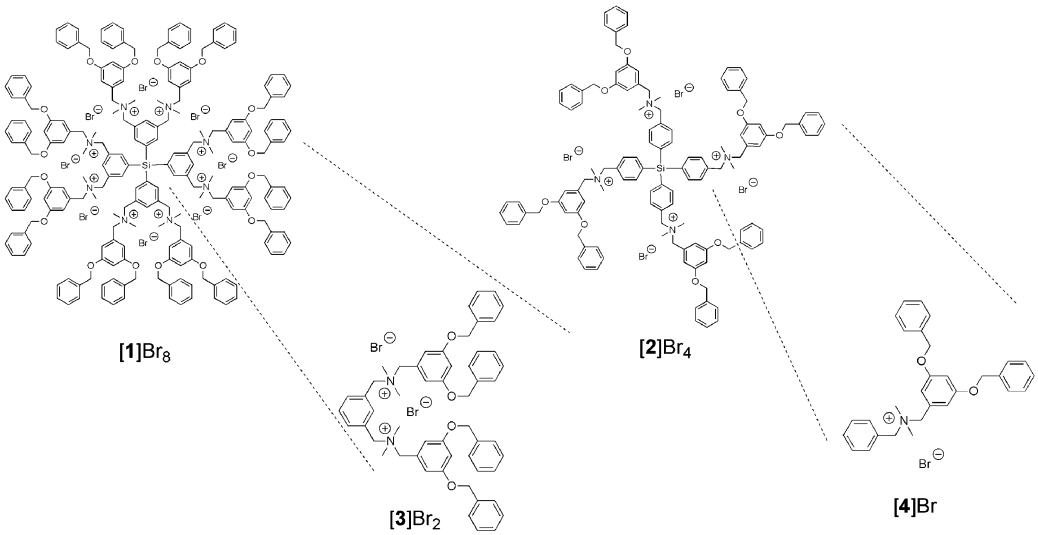

Fig. 1 Octa-cationic and tetra-cationic core–shell dendrimers $[\mathbf{1}]^{8+}$ and $[\mathbf{2}]^{4+}$, and di-cationic and mono-cationic wedges $[\mathbf{3}]^{2+}$ and $[\mathbf{4}]^{+}$ bearing eight, four, two and one bromide ion(s) as counterion(s), respectively.

molecules. In addition, the substrate selectivity of octa-ionic dendrimer [**1**]Br_8 and dendritic wedges [**3**]Br_2 and [**4**]Br is investigated by means of substrate competition experiments.

Experimental

General comments

Diethyl ether was dried over sodium using benzophenone as indicator. Dichloromethane was dried over CaH_2. Both solvents were distilled prior to use. *N*,*N*-Dimethylbenzylamine (**7**), Methyl Orange and methyl iodide were purchased from Acros Chimica or Aldrich and used without further purification. Dendron [G1]-Br (**5**)[9] and 1,3-bis[(dimethylamino)-methyl]benzene (**6**),[10] were prepared according to literature procedures. ^1H and $^{13}C\{^1H\}$ NMR spectroscopic measurements were carried out on a Varian Inova/Mercury 300 or 200 MHz spectrometer at 25 °C and chemical shifts (δ) are given in ppm referenced to the residual solvent peak. The MALDI-TOF mass spectra were acquired using a Voyager-DE Bio-spectrometry workstation mass spectrometer (PerSeptive Bio-systems Inc., Framingham, MA, USA). Dornis and Kolbe, Mikroanalytische Laboratorium, Mülheim a/d Ruhr, Germany performed the elemental analyses.

Syntheses

[3]Br_2. A solution of 1,3-[(dimethylamino)methyl]benzene (**6**) (0.4 g, 2.08 mmol) and [G1]-Br (**5**) (1.6 g, 4.23 mmol) in CH_2Cl_2 (15 mL) was stirred overnight, whereupon the mixture was concentrated *in vacuo*. The resultant white product was washed with diethyl ether (3 × 25 mL) to remove the slight excess of [G1]-Br. Compound [**3**]Br_2 was obtained as a white

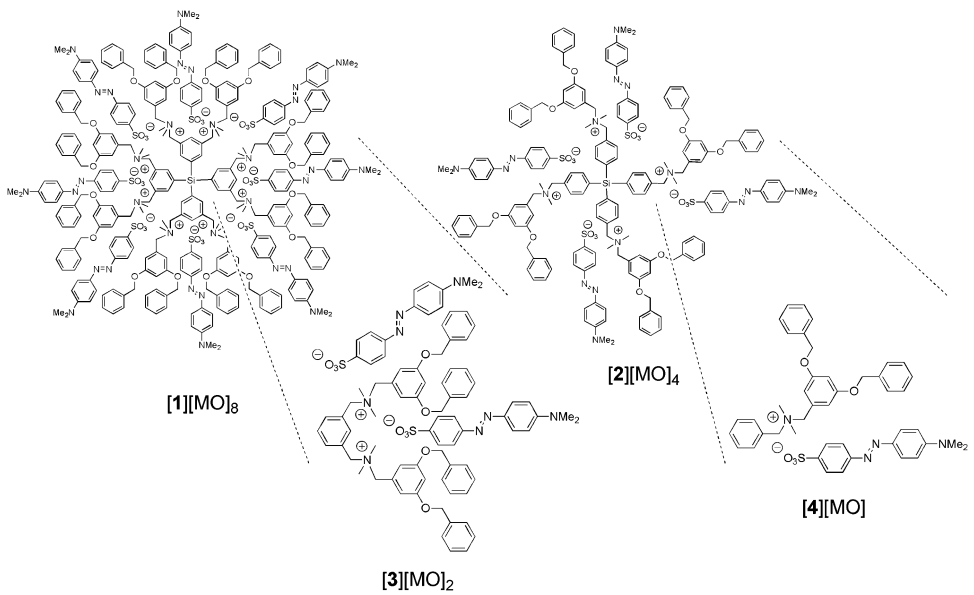

Fig. 2 Dendritic MO host–guest assemblies [**1**][MO]$_8$, [**2**][MO]$_4$, [**3**][MO]$_2$ and [**4**][MO].

powder in 84% yield. ^{1}H NMR ($CDCl_3$): δ 8.28 (br s, 1H; *meta*-ArH), 7.77 (d, ^3J(H,H) = 8 Hz, 2H; *ortho*-ArH),), 7.61 (br d, ^4J(H,H) = 6.4 Hz, 1H; *ortho*-ArH), 7.45–7.19 (m, 20H; ArH), 6.91 (s, 4H; ArH), 6.64 (s, 2H; ArH), 5.08 (br s, 4H; CH_2N), 5.01 (s, 8H; OCH_2), 4.92 (br s, 4H; NCH_2), 3.03 (br s, 12H; NMe); ^{13}C{^{1}H} NMR ($CDCl_3$): δ 160.1, 136.4, 135.6, 129.1, 128.8, 128.3, 128.0 (Ar), 112.6, 104.6 (Ar), 70.6 (OCH_2), 68.1 and 67.5 (CH_2NCH_2), 49.2 (NMe_2); elemental analysis. calc. (%) for $C_{54}H_{58}Br_2N_2O_4$ (958.86): C 67.64, H 6.10, N 2.92; found: C 67.69, H 6.15, N 2.90.

[3][MO]$_2$. A biphasic system of [**3**]Br_2 (0.34 g, 0.36 mmol) in CH_2Cl_2 (100 mL) and the sodium salt Methyl Orange (0.16 g, 0.49 mmol) in deionized water (150 mL) was strirred overnight. The organic layer was separated off, washed with deionized water (5 × 100 mL) until the water layer was colorless, concentrated, and dried *in vacuo*. Compound [**3**][MO]$_2$ (0.28 g; 0.20 mmol) was isolated as an orange powder in 78% yield. ^{1}H NMR ($CDCl_3$): δ 8.30 (br s, 1H; ArH), 8.00 (d, ^3J(H,H) = 8.1 Hz, 4H; ArH(MO)), 7.82 (d, ^3J(H,H) = 8.7 Hz, 4H; ArH(MO)), 7.75 (d, ^3J(H,H) = 8.1 Hz, 4H; ArH (-MO)), 7.68 (d, ^3J(H,H) = 6.6 Hz, 2H; ArH), 7.4–7.2 (m, 21H; ArH), 6.76 (s, 4H; ArH), 6.70 (d, ^3J(H,H) = 9.3 Hz, 2H; ArH(MO)), 6.60 (s, 2H; ArH), 4.93 (s, 8H; OCH_2), 4.87 (br s, 4H; CH_2N), 4.68 (br s, 4H; NCH_2), 3.06 (s, 12H; NMe_2(MO)), 2.90 (br s, 12H; NMe_2); ^{13}C{^{1}H} NMR ($CDCl_3$): δ 159.8 (Ar), 153.4, 152.4, 146.9, 143.4 (q-Ar(MO)), 138.5, 136.2, 135.2, 130.5, 129.9, 129.3, 128.9, 128.4, 127.9 (Ar), 126.6, 125.1, 122.0 (Ar(MO)), 112.1 (Ar), 111.4 (Ar(MO)), 104.4 (Ar), 70.1 (OCH_2), 68.0 (br s, CH_2NCH_2), 48.6 (NMe_2), 40.2 (br, NMe_2(MO)); elemental analysis: calc. (%) for $C_{82}H_{86}N_8O_{10}S_2$ (1407.74): C 69.96, H 6.16, N 7.96; found: C 70.10, H 6.26, N 8.05.

[4]Br. A solution of *N*,*N*-dimethylbenzylamine (**7**) (0.24 mg, 1.92 mmol) and [G1]-Br (**5**) (0.78 mg, 1.98 mmol) in CH_2Cl_2 (40 mL) was stirred overnight, whereupon the mixture was concentrated *in vacuo*. The crude product was redissolved in CH_2Cl_2 (10 mL) to precipitate with Et_2O (75 mL). The residue was washed with diethyl ether (3 × 75 mL) to remove the slight excess of [G1]-Br. Compound [**4**]Br was quantitatively isolated as a white powder. ^{1}H NMR ($CDCl_3$): δ 7.6–7.2 (m, 15H; ArH), 6.84 (d, ^4J(H,H) = 2.2 Hz, 2H; ArH), 6.70 (t, ^4J(H,H) = 2.0 Hz, 1H; ArH), 5.08 (s, 2H; CH_2O), 4.95 (s, 2H; CH_2N), 4.87 (s, 2H; NCH_2), 2.98 (s, 6H; NMe_2); ^{13}C{^{1}H} NMR ($CDCl_3$): δ 160.2, 136.5, 133.5, 131.0, 129.4, 128.8, 128.3, 127.9, 127.3, 112.5, 104.8 (Ar), 70.5 (CH_2O), 68.6 (CH_2N), 68.1 (NCH_2), 48.8 (NMe_2) (one aryl carbon not resolved); elemental analysis: calc. (%) for $C_{30}H_{32}BrNO_2$ (518.48): C 69.50, H 6.22, N 2.70; found: C 69.32, H 6.07, N 2.66.

[4][MO]. A biphasic system of [**4**]Br (0.35 g, 0.68 mmol) in CH_2Cl_2 (100 mL) and Methyl Orange (0.26 g, 0.81 mmol) in deionized water (300 mL) was stirred for 2 h. The organic layer was separated off, washed with deionized water (3 × 200 mL), and dried *in vacuo*. Compound [**4**][MO] was isolated as an orange powder in quantitative yield. ^{1}H NMR (CD_2Cl_2): δ 8.03 (d, ^3J(H,H) = 8.4 Hz, 2H; ArH(MO)), 7.86 (d, ^3J(H,H) = 8.7 Hz, 2H; ArH(MO)), 7.80 (d, ^3J(H,H) = 8.1 Hz, 2H; ArH(MO)), 7.5–7.2 (m, 15H; ArH). 6.78 (d, ^4J(H,H) = 2.1 Hz, 2H; ArH), 6.67 (t, ^4J(H,H) = 2.1 Hz, 1H; ArH), 5.04 (s, 4H; OCH_2), 4.83 (s, 2H; CH_2N) 4.72 (s, 2H; NCH_2), 3.09 (s, 6H; NMe_2(MO)), 2.91 (s, 6H; NMe_2); ^{13}C{^{1}H} NMR (CD_2Cl_2): δ 162.1 (Ar), 155.5, 154.8, 149.9, 145.5 (q-Ar(MO)), 138.7, 135.3, 132.3, 131.4, 131.2, 130.5, 130.4, 130.0, 129.8, 129.5 (Ar), 128.8, 127.1, 123.9 (Ar(MO)), 114.4 (Ar), 113.5 (Ar(MO)), 72.2 (OCH_2), 70.6 (CH_2N), 70.2 (NCH_2), 50.4 (NMe_2(MO)), 42.1 (NMe_2); MS (MALDI-TOF, 9-nitroanthracene): *m*/*z*: 1923.76 [3M − MO]$^+$, 1179.36 [2M − MO]$^+$, 436.22 [M−MO]$^+$; elemental analysis: calc. (%) for $C_{44}H_{46}N_4O_5S$ (742.93): C 71.13, H 6.24, N 7.54; S 4.32 found: C 71.18, H 6.28, N 7.39, S 4.39.

Substrate competition experiment

A typical experiment is as follows: A solution of sodium *p*-tolylsulfonate (**C**) (16.9 mg, 87 μmol) and potassium *p*-tolylcarboxylate (**D**) (16.1 mg, 92 μmol) in deionized water (5 mL) and a solution of [**1**]Br_8 (40.0 mg, 7.8 μmol) in dichloromethane (5 mL) were put together to form a biphasic system. This biphasic system was stirred overnight at room temperature. The organic layer was separated and washed with deionized water (5 × 10 mL). The organic layer was then concentrated *in vacuo* to give a white product, which was analyzed by ^{1}H NMR spectroscopy. From the peak integration data the total exchange could be calculated as well as the exchange of each of the substrate molecules.

Crystal structure determinations

X-Ray intensities were collected on a Nonius KappaCCD diffractometer with rotating anode and Mo-Kα radiation (graphite monochromator, λ = 0.71073 Å). The structures were solved with Direct Methods (SHELXS-97[11] for [**3**]Br_2, SIR-97 [12] for [**4**][MO]) and refined with SHELXL-97[11] against F^2 of all reflections. The drawings, structure calculations, and checking for higher symmetry were performed with the program PLATON.[13]

[3]Br_2. $C_{54}H_{58}N_2O_4{}^{2+}(Br^-)_2$ + disordered solvent, M = 958.84,[14] colorless block, 0.21 × 0.18 × 0.09 mm^3. Trigonal crystal system, space group $R\bar{3}$ (no. 148). Cell parameters: a = b = 37.1517(5), c = 19.4231(3) Å, V = 23 217.0(6) Å^3. Z = 18, D_c = 1.234 g cm^{-3},[14] μ = 1.615 mm^{-1}.[14] 33 681 reflections were measured at 150(2) K up to a resolution of $(\sin\theta/\lambda)_{max}$ = 0.48 Å^{-1}. An absorption correction based on multiple measured reflections was applied (SortAV, correction range 0.75–0.97). 4799 reflections were unique (R_{int} = 0.0740), of which 3558 were observed [$I > 2\sigma(I)$]. The benzyl group at O4 was refined with two disorder components and isotropic displacement parameters, constrained to a regular hexagon. All other non-hydrogen atoms were refined with anisotropic displacement parameters. The crystal structure contained large voids (2117 Å^3 per unit cell) filled with disordered solvent molecules, amounting to 815 electrons per unit cell. Their contribution to the structure factors was secured by back-Fourier transformation with the SQUEEZE procedure in the program PLATON.[13] 529 refined parameters, 3 restraints. R (obs. refl.): $R1$ = 0.0586, $wR2$ = 0.1749. R (all data): $R1$ = 0.0758, $wR2$ = 0.1881. Weighting scheme $w = 1/[\sigma^2(F_o^2) + (0.1232P)^2 + 47.8216P]$, where $P = (F_o^2 + 2F_c^2)/3$.

GoF = 1.082. Residual electron density between −0.41 and 1.87 e Å^{-3}.

[4][MO]. $[C_{30}H_{32}NO_2]^+[C_{14}H_{14}N_3O_3S]^- \cdot 2.5C_6H_6$, M = 938.18, orange plate, 0.36 × 0.36 × 0.15 mm^3. Triclinic crystal system, space group $P\bar{1}$ (no. 2). Cell parameters: a = 9.9322(2), b = 13.9718(2), c = 19.3040(4) Å, α = 100.3272(10), β = 92.3451(8), γ = 103.8291(9)°, V = 2549.18(8) Å^3. Z = 2, D_c = 1.222 g cm^{-3}, μ = 0.117 mm^{-1}. 34 970 reflections were measured at 110(2) K up to a resolution of $(\sin\theta/\lambda)_{max}$ = 0.65 Å^{-1}. An absorption correction was not considered necessary. 11 536 reflections were unique (R_{int} = 0.0511), of which 8939 were observed [$I > 2\sigma(I)$]. The Methyl Orange molecule was refined with a stilbene-type disorder model; one benzene solvent molecule was rotationally disordered about the sixfold axis. Non-hydrogen atoms were refined with anisotropic displacement parameters, hydrogen atoms were refined as rigid groups. 808 refined parameters, 123 restraints. R (obs. refl.): $R1$ = 0.0433, $wR2$ = 0.1055. R (all data): $R1$ = 0.0604, $wR2$ = 0.1142. Weighting scheme $w = 1/[\sigma^2(F_o^2) + (0.0507P)^2 + 0.6051P]$, where $P = (F_o^2 + 2F_c^2)/3$. GoF = 1.026. Residual electron density between –0.39 and 0.23 e Å^{-3}.

CCDC reference numbers 644298 and 644299.

For crystallographic data in CIF or other electronic format see DOI: 10.1039/b617669k

Results

Synthesis and characterization of model compounds [3]Br_2, [3][MO]$_2$, [4]Br and [4][MO]

In a recent study,[6] the X-ray crystal structure of a representative model species for the octa-ionic core of dendrimer [**1**]Br_8 showed that anions can be accommodated inside the dendritic structure by means of ion pair formation with the ammonium sites at the dendrimer core. Regrettably, all attempts to crystallize the dendrimers [**1**]Br_8 and [**2**]Br_4 as well as their corresponding MO assemblies failed. This prompted us to synthesize smaller 'model' compounds, which resemble specific sections of the ionic core–shell dendrimer, as well as their MO host–guest assemblies. The dendritic wedges [**3**]Br_2 and [**4**]Br, and their MO assemblies [**3**][MO]$_2$ and [**4**][MO] were prepared from dendron G1-Br (**5**)[9] and 1,3-bis[(dimethylamino)methyl]-benzene (**6**)[10] and *N*,*N*-dimethylbenzylamine (**7**), respectively (Scheme 1). Dendron **5** contains a benzylic bromide group at the focal point, which was used for the quantitative quaternization of the amino groups of **6** and **7**. This afforded [**3**]Br_2 and [**4**]Br as white solids in 84% and quantitative yield, respectively. Alike dendrimers [**1**]Br_8 and [**2**]Br_4, both ionic wedges are soluble in organic solvents such as dichloromethane, but are insoluble in water.

To a solution of [**3**]Br_2 or [**4**]Br in dichloromethane was added a slight excess of Methyl Orange (Na[MO]) in water. The resulting biphasic set-ups were vigorously stirred, which resulted in an instantaneous colorization of the organic layers. The formation of these orange-colored organic layers indicates that exchange of the bromide anions of [**3**]Br_2 and [**4**]Br for

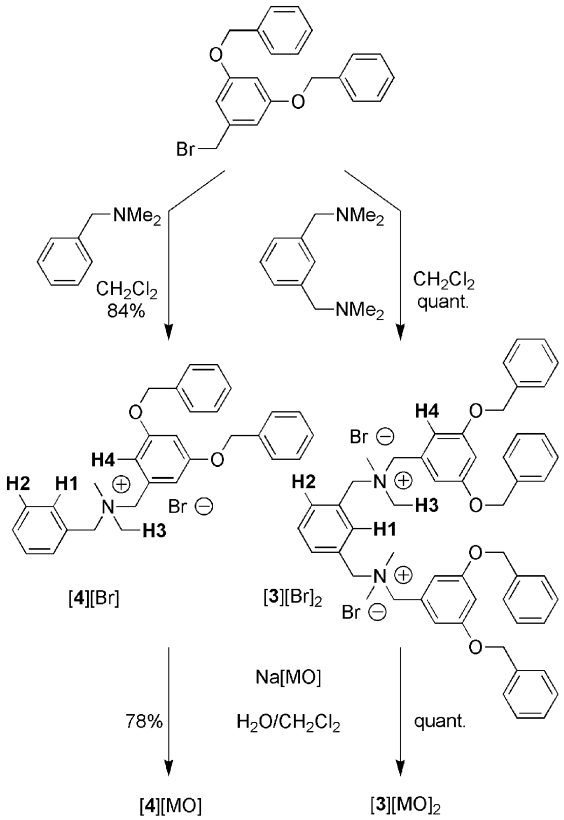

Scheme 1 Synthesis of ionic dendritic wedges [**3**]Br_2 and [**4**]Br, and their corresponding MO assemblies [**3**][MO]$_2$ and [**4**][MO] (including numbering scheme for Table 1).

MO had occurred since Na[MO] is insoluble in dichloromethane. The organic phases were washed with water to remove formed sodium bromide, which afforded MO assemblies [**3**][MO]$_2$ and [**4**][MO] as orange solids in 78% and quantitative yield, respectively.

The NMR spectra and elemental analysis of [**3**][Br]$_2$ and [**4**][Br], and their corresponding MO assemblies [**3**][MO]$_2$ and [**4**][MO] are in full agreement with the proposed structures in Fig. 1 and 2. Specific peak integration in the ^{1}H NMR spectra of [**3**][MO]$_2$ and [**4**][MO] showed that quantitative exchanges of bromide anions had been achieved. Diagnostic shifts were observed in the ^{1}H NMR spectra of the MO assemblies [**3**][MO]$_2$ and [**4**][MO] compared to wedges [**3**]Br_2 and [**4**]Br (Table 1). Significant upfield shifts of 0.07–0.15 ppm were found for the protons of the NMe_2 and aryl groups of the dendritic inner shell. Similar changes in chemical shift values were found for dendrimers [**1**]Br_8 and [**2**]Br_4 upon formation of MO assemblies [**1**][MO]$_8$ and [**2**][MO]$_4$.[6] The changes in chemical shift values of the wedges are, however, smaller than the shifts observed for the dendrimers. In the case of [**3**]Br_2, a downfield shift was observed for aryl proton H2 at the focal point of the wedge, whereas an upfield shift was found for proton H2 in the tetraphenylsilane group of the core unit of the dendrimer. The structural aspects of diionic wedge [**3**]Br_2 and MO assembly [**4**][MO] were further investigated by X-ray crystal structure determination.

Table 1 Selected ^{1}H NMR spectroscopic data of [**1**]Br_8, [**2**]Br_4, [**3**]Br_2 and [**4**]Br and their corresponding MO assemblies[a]

Dendrimer[b]	H1, H2	H4	H3
[**1**]Br_8	8.19, 8.41	7.00	3.07
[**1**][MO]$_8$	8.75, 8.88	6.67	2.78
[**2**]Br_4	7.77 (d)	6.73	2.98
[**2**][MO]$_4$	7.76 (br)	6.71	2.83
Wedge	H1, H2	H4	H3
[**3**]Br_2	8.28, 7.77 (d)	6.91	3.03
[**3**][MO]$_2$	8.30, 7.68 (d)	6.76	2.90
[**4**]Br	7.6–7.2 (m)	6.84	2.98
[**4**][MO][c]	7.5–7.2 (m)	6.78	2.91

[a] All samples (10^{-3} M) were analyzed in $CDCl_3$. The chemical shifts are listed in ppm and signals are singlet resonances unless stated otherwise. Abbreviations used: d = doublet, m = multiplet, br = broad signal, MO = Methyl Orange anion. [b] Data taken from ref. 6. [c] Analyzed in CD_2Cl_2.

X-Ray crystal structure of [3]Br_2

Colorless, block-shaped, single crystals suitable for X-ray analysis were obtained by layering a dichloromethane solution of [**3**]Br_2 with diethyl ether. In the molecular structure of [**3**]Br_2 the dendritic arms are located at the same side of the central phenyl ring (1) at the focal point of the wedge (Fig. 3). The distances between the center of ring (1) (Cg(1))[15] and the terminal carbon atoms C(21), C(28), C(45) and C(52B) are 12.76(2), 11.524(14), 12.083(11) and 12.471(17) Å, respectively. The molecule has approximate mirror symmetry with the mirror bisecting the focal point. Especially about phenyl rings (2) and (5) the conformation is comparable (Table 2). At the end of the wedge, phenyl rings (4) and (6) are located at a relatively short distance (4.584(7) Å) from each other. It should be noted that the refinement of one of the phenyl end groups, *i.e.* ring (7), was troublesome due to conformational disorder in this part of the molecular structure.

Table 2 Selected torsion angles (°) of [**3**]Br_2 with s.u's (standard uncertainties) in parentheses

C(2)–C(1)–C(7)–N(1)	−86.8(8)	C(2)–C(3)–C(31)–N(2)	92.0(8)
C(10)–N(1)–C(7)–C(1)	−53.8(8)	C(32)–N(2)–C(31)–C(3)	−67.0(7)
C(7)–N(1)–C(10)–C(11)	−168.8(6)	C(31)–N(2)–C(34)–C(35)	164.2(6)
N(1)–C(10)–C(11)–C(12)	102.5(8)	N(2)–C(34)–C(35)–C(36)	−102.6(7)

Bromide anions Br(1) and Br(2) are located at two distinctive binding sites of the dendritic wedge (Fig. 4). Br(1) is embedded in a cleft formed by the ammonium groups and the two dendritic arms of the wedge. The distances between Br(1) and nitrogen atoms N(1) and N(2) of the ammonium groups amount to 4.350(7) and 4.353(6) Å, respectively (Table 3). Relatively short distances were found between Br(1) and hydrogen atoms of the ammonium groups and phenyl rings (2) and (5) of the dendritic wedge.[16] The shortest distances were found for Br(1)···H(32B) (2.72 Å), Br(1)···H(34A) (2.82 Å), and Br(1)···H(16) (2.92 Å). Interestingly, Br(1) is located above the ring centroid Cg(1). The angle defined by Br(1), Cg(1) and C(1) is 87.4(3)°, while the distance between Br(1) and Cg(1) is 4.222(3) Å.

The second bromide anion Br(2) is located beside the dendritic wedge. Br(2) is, in fact, located in a pocket formed by two adjacent dicationic wedges at distances of 4.176(7) and 4.096 Å from nitrogen atom N(1) and N(2) of an adjacent wedge, respectively (Fig. 4, Table 3). Short distances were found between Br(2) and hydrogen atoms of the ammonium CH_2 and CH_3 groups and phenyl rings (1), (5) and (2) of an adjacent wedge. The shortest distances were found for Br(2)···H(6) (2.99 Å), Br(2)···H(9B) (2.85 Å), and Br(2)···H(10A) (2.77 Å). In addition, the distances between Br(2) and hydrogen atoms H(34A) and H(31B) of an ammonium group amount to 2.85 and 2.71 Å, respectively.

X-Ray crystal structure of assembly [4][MO]

MO assembly [**4**][MO] was crystallized as orange-colored crystalline plates from a saturated benzene solution. The

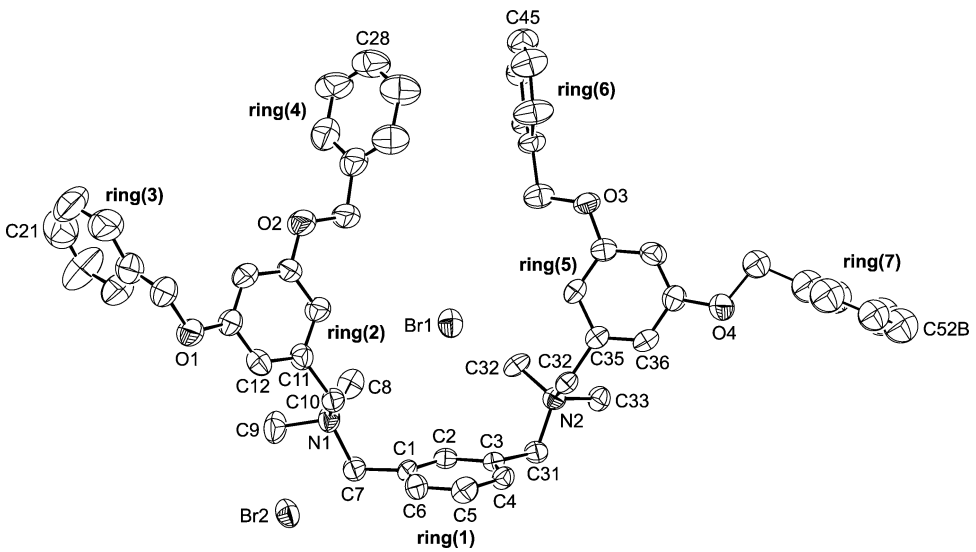

Fig. 3 Displacement ellipsoid plot of [**3**]Br_2 drawn at the 50% probability level. Only the major disorder component of ring (7) is shown. Hydrogen atoms and disordered solvent molecules are omitted for clarity.

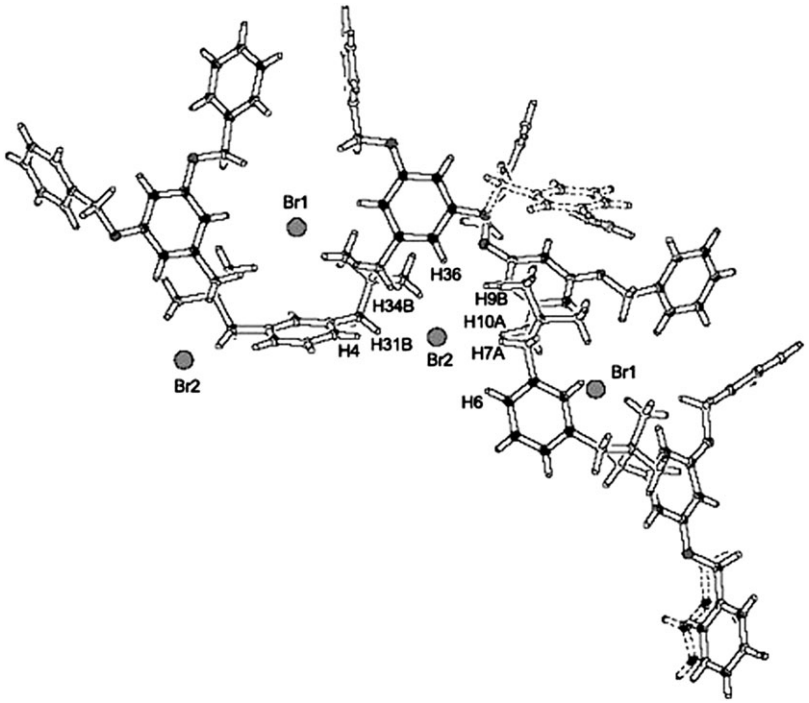

Fig. 4 Molecular plot of two adjacent wedges [**3**]Br_2 with adopted numbering scheme.

molecular structure of [**4**][MO] shows a 1 : 1 assembly between the monocationic dendritic wedge [**4**]$^+$ and an MO anion (Fig. 5). The distance between the carbon atoms C(283) and C(183), which are located at two different ends of the dendritic wedge, amounts to 12.529(2) Å. The MO anion is positioned with its NMe_2 group close to C113 of the wedge and its sulfonato group in the proximity of the ammonium group. The shortest intermolecular distance between the oxygen atoms of the sulfonato group and the nitrogen atom of the ammonium group is O(31)···N(3) 4.5538(15) Å, while the other distances are O(31)···N(3) 6.1821(15) Å and O(21)···N(3) 6.7281(15) Å (*vide infra*).

The planes of the phenyl rings of the MO anion are twisted (9.4°) to one another (Table 4). The MO anion is slightly curved (torsion angle C(11)–N(11)–N(21)–C(71) 177.0(3)°), which gives rise to disorder of MO anions in the crystal packing (Fig. 6). For clarity we have only displayed the MO anion that is most abundant in the crystal in Fig. 5. In the crystal, the MO anions are arranged as discrete dimers (Fig. 7). The MO–MO dimers are separated by dendritic wedges. The sulfonato groups of the MO anions are directed to opposite directions of the MO–MO dimer, which displays a coplanar, offset geometry with an interplanar separation of 3.545 Å. The dihedral angle between the plane defined by phenyl ring (5) and the plane defined by phenyl ring (5)* of a second MO anion is 0.03°. One phenyl ring is offset relative to the other by 23.3°.

The X-ray crystal structure of [**4**][MO], furthermore, shows that phenyl rings (2) and (6) of the benzyl aryl ether moiety of the dendritic wedge reside in one plane (Fig. 5 and Table 3). The azobenzene moiety of MO displays an edge-to-face relationship with the planar benzyl aryl ether moiety of the wedge. Remarkably, this edge-to-face arrangement has an L-shaped geometry, rather than T-shaped. A relatively short distance of 2.72 Å was found for H(91) connected to C(91) on ring (5) of MO and ring centroid Cg(6) of the planar benzyl aryl ether unit of the wedge (Fig. 5 and 6).

The oxygen atoms of the sulfonato group of two neighboring MO anions, denoted as MO(b) and MO(d), are located at relatively short distances from methyl and benzyl hydrogen atoms of the ammonium group and phenyl rings (2) and (8) of the dendritic wedge (Fig. 8 and Table 5). The shortest distances were observed for H(21B)···O(11)b (2.39 Å), H(22B)···O(11)d (2.53 Å), H(24B)···O(21)b (2.40 Å) and H(43)···O(31)d (2.54 Å). In these specific cases, the angle defined by the carbon, the hydrogen, and the oxygen atom ranges between 146 and 162°.

Binding properties of ionic core–shell dendrimers

The incorporation of MO into a polycationic core–shell dendrimer is performed in a biphasic set-up of water and dichloromethane. As a consequence of this set-up, the incorporation of multiple guest molecules involves several processes, *i.e.* phase-transfer reactions of anions between the water phase and the dichloromethane phase as well as exchange of anionic guest molecules and bromide anions of the ionic core–shell dendrimer. In order to study the incorporation of guest molecules in more detail the anion exchange reaction with MO was carried out in a single phase, *i.e.* in dichloromethane. In this set-up, effects related to phase-transfer reactions are excluded, which enables us to focus on the exchange of MO and Br anions. In theory, each MO guest has its own binding constant. For simplicity, the first experiments were performed with the tetraionic dendrimer [**2**]Br_4 (Fig. 1), which was reacted with the tetrabutylammonium salt of MO, [NBu_4][MO], in a single-phase anion exchange experiment in

Table 3 Selected intermolecular distances (Å) and angles (°) of [**3**]Br_2 with s.u's in parentheses[11]

Interatomic distances					
Br(1)···H(10B)	2.94		Br(2)···H(36)[a]	3.08	
Br(1)···H(40)	2.96		Br(2)···H(31B)[a]	3.02	
Br(1)···H(32A)	3.01		Br(2)···H(4)[a]	3.18	
Br(1)···N(1)	4.530(7)		Br(2)···H(47)[b]	2.99	
Br(1)···N(2)	4.353(6)		Br(2)···N(1)	4.176(7)	
Br(1)···Cg(1)	4.222(3)		Br(2)···N(2)[a]	4.096(8)	
Br(2)···H(6)	2.99		Br(1)···H(44)[c]	3.02	
Br(2)···H(7A)	3.03		Br(2)···H(31B)[a]	3.02	
Short ring interactions					
Cg(I) → Cg(J)	Cg(I)–Cg(J)[g]	α[h]	β[i]	γ[j]	Cg(I)···perp[k]
Cg(4) → Cg(6)	4.584(7)	46.65	46.68	2.79	4.579
X–H···π interactions					
X(I)–H(I) → Cg(J)	H···Cg[l]	H···perp[m]	γ[n]	X–H···Cg[o]	X···Cg[p]
C(29)–H(29) → Cg(6)	3.24	2.86	28.16	111	3.693(16)
Potential H bonds					
D–H···A	D–H	H···A	D···.A	D–H···A	
C(9)–H(9B)···Br(2)[d]	0.98	2.86	3.724(8)	148	
C(10)–H(10A)···Br(2)	0.99	2.77	3.727(8)	162	
C(16)–H(16)···Br(1)	0.95	2.92	3.660(11)	135	
C(19)–H(19)···O(1)	0.95	2.39	2.782(14)	104	
C(32)–H(32B)···Br(1)	0.98	2.72	3.673(8)	164	
C(34)–H(34A)···Br(1)[e]	0.99	2.85	3.761(7)	153	
C(34)–H(34B)···Br(2)[f]	0.99	2.72	3.648(6)	157	

[a] Symmetry operations: a1 $y-1/3, 1/3-x+y, 1/3-z$. [b] a2: $x-y, x, -z$. [c] a3: $2/3-x, 1/3-y, 1/3-z$. [d] a4: $1/3-x, 2/3-y, 2/3-z$. [e] a5: $2/3-y, 1/3+x-y, 1/3+z$. [f] a6: $2/3+x-y, 1/3+x, 1/3-z$. [g] Distance between ring centroids (Å). [h] Dihedral angle between planes I and J (°). [i] Angle between Cg(I) → Cg(J) vector and normal to plane J (°). [j] Angle between Cg(I) → Cg(J) vector and normal to plane I (°). [k] Perpendicular distance of Cg(I) on ring J. [l] Distance between H(I) and ring centroid Cg(J) (Å). [m] Perpendicular distance of H(I) on ring J (Å). [n] Angle between H(I) → Cg(J) vector and normal to plane J (°). [o] Angle defined by X(I), H(I), and Cg(J) (°). [p] Distance between X(I) and Cg(I) (Å).

dichloromethane. In an attempt to determine the binding constant for the binding of the first MO guest in CD_2Cl_2 an NMR titration experiment was performed. The changes of the proton resonances of the MO anion and the dendritic host cation were monitored in a 3.9×10^{-3} M host solution with addition of a solution of [NBu_4][MO] (8.3×10^{-3} M) in the same host concentration, thereby keeping the host concentration constant. The fact that only minor changes (<0.02 ppm) of the resonances of MO guest and dendritic host proton resonances were recorded rendered nonlinear regression analysis impossible. The ^{1}H NMR spectrum at −90 °C of the final solution of [**2**]Br_4 and [NBu_4][MO] in a 1 : 1 ratio showed broadened peak resonances, but no sign of decoalesence, which suggest that the exchange of MO and Br anions in a single phase is fast on the NMR time scale.

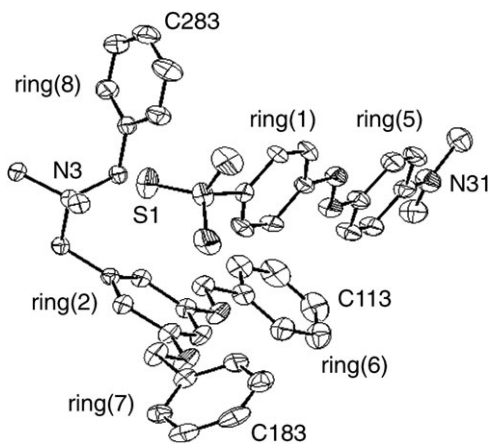

Fig. 5 Displacement ellipsoid plot (50% probability) of host–guest assembly [**4**][MO]. Solvent molecules and hydrogen atoms have been omitted for clarity.[17]

Table 4 Selected distances (Å) and torsion angles (°) of the assembly [**4**][MO] with s.u's in parentheses

Bond distances			
S(1)–O(11)	1.4544(11)	S(1)–O(21)	1.4442(11)
S(1)–O(31)	1.4440(10)		

Torsion angles			
C(73)–O(13)–C(13)–C(63)	0.24(18)	N(21)–N(11)–C(11)–C(21)	1.8(4)
C(13)–O(13)–C(73)–C(83)	178.77(11)	C(11)–N(11)–N(21)–C(71)	177.0(3)
O(13)–C(73)–C(83)–C(93)	−171.89(12)	N(11)–N(21)–C(71)–C(81)	−174.3(4)
O(11)–S(1)–C(41)–C(51)	−137.6(5)	C(131)–N(31)–C(101)–(91)	4.7(18)

In addition, UV titration experiments were carried out to determine the binding constants of the four MO guests. Dilution experiments revealed, however, that [NBu_4][MO] self-aggregates in dichloromethane at a concentration of 10^{-5} M.[18] The self-aggregation of MO seriously complicates

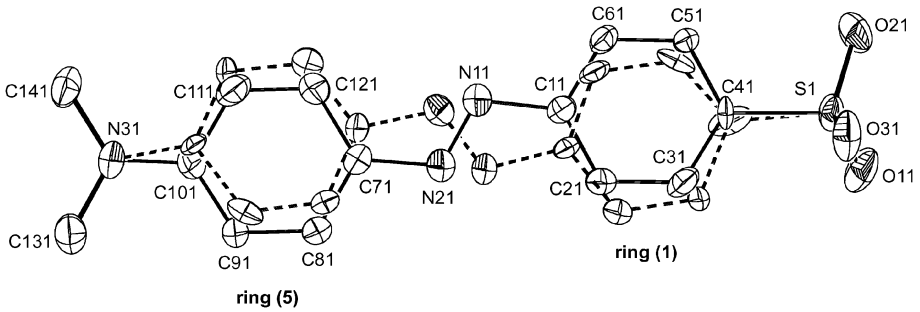

Fig. 6 Displacement ellipsoid plot (50% probability) of the disordered MO anion (structural fragments 0 and 1) of [**4**][MO] with adopted numbering scheme. The major disorder component (67.3% occupancy) is drawn with solid lines, the minor component (32.7% occupancy) with dashed lines.[17]

the interpretation of the titration curves. The titration curve, in fact, displays a combination of various equilibria, *i.e.* MO self-aggregation and the exchange equilibria of four MO between [NBu_4][MO] and [**2**]Br_4. Due to these limitations, we were not able to determine a reliable binding constant for MO to a polyionic core–shell dendrimer.

Substrate selectivity studies

The influence of the molecular structure of the anionic guest molecules on their non-covalent binding by the polyionic core–shell dendrimers in a biphasic set-up was investigated. The substrate selectivity of octaionic dendrimer [**1**]Br_8 and ionic wedges [**3**]Br_2 and [**4**]Br was investigated by means of preliminary substrate competition experiments with the four substrate molecules depicted in Fig. 9. The substrate molecules comprise either a sulfonato or carboxylato group, and an organic moiety, which is either a methyl or *p*-tolyl group. The influence of the different parts on the non-covalent binding of substrate molecules by the dendritic hosts was studied.

In a typical competition experiment, a solution of the ionic dendrimer or a dendritic wedge in dichloromethane was treated with a solution of alkali salts of two substrate molecules, *i.e.* **A** and **B** or **C** and **D**, in water. A slight excess of each substrate molecule with respect to the number of ammonium groups of the dendritic species was used. The alkali salts of the anionic substrate molecules are soluble in water, but insoluble in dichloromethane. After thorough stirring of the biphasic set-ups, the organic layers were separated off and analyzed by ^{1}H NMR spectroscopy. The number of exchanged anions was determined by selective peak integration (Table 6). In case of methyl sulfonate (**A**) and acetate (**B**), no anion exchange had occurred, whereas in the competition experiment between *p*-toluenesulfonate (**C**) and *p*-methyl benzoate (**D**), anion exchange did occur. In contrast with the earlier anion exchange reactions carried out with MO,[6] which showed a quantitative exchange of bromide anions for MO anions, in the present cases 81–86% of the bromide anions were exchanged for substrate molecules **C** and **D**. Dendrimer [**1**]Br_8 as well as wedges [**3**]Br_2 and [**4**]Br showed preferential binding for *p*-toluenesulfonate (**C**) over *p*-carboxylate **D** (Table 6).

In order to further investigate the influence of the shell on the binding properties of an ionic core–shell dendrimer, dendrimer [**9**]Br_8 was additionally tested on its binding selectivity. Dendrimer [**9**]Br_8 differs from dendrimer [**1**]Br_8 in that [**9**]Br_8 has its inner shell of aryl ether groups decorated with apolar dodecyl groups (Fig. 10).[19] A slightly more pronounced substrate binding efficiency and selectivity (for **C**) was observed

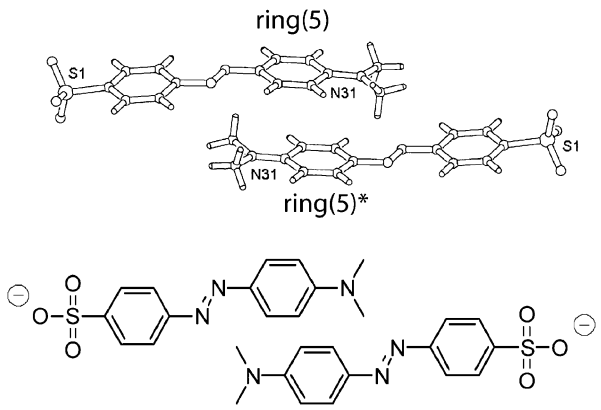

Fig. 7 Molecular plot of a MO–MO dimer present in the crystal structure of [**4**][MO].

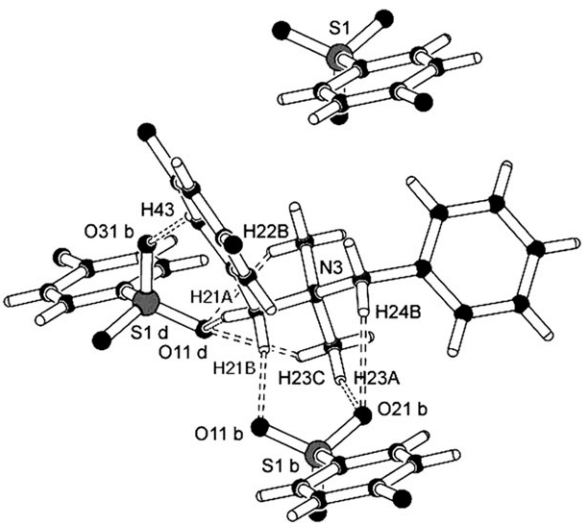

Fig. 8 Molecular plot of the ammonium site of [**4**][MO] and neighbouring MO anions MO(b) and MO(d). The dashed lines show the shortest distances observed between the oxygens of the sulfonato group of MO and methyl, benzylic protons and aryl protons of [**4**].

Table 5 Selected intermolecular distances and angles of the assembly [**4**][MO] formed between dendritic moiety [**4**]$^+$ and the MO anion, with s.u.'s in parentheses[11]

Short ring interactions					
Cg(I) → Cg(J)	Cg(I)–Cg(J)[a]	α[b]	β[c]	γ[d]	Cg(I)···perp[e]
Cg(2) → Cg(1)	5.197	74.79	10.63	69.76	1.798
Cg(6) → Cg(5)	4.736	72.25	10.49	76.53	1.103
Cg(5) → Cg(5)[f]	3.861	0.03	23.33	23.33	3.545

X–H···π interactions					
X(I)–H(I) → Cg(J)	H···Cg[g]	H···perp[h]	γ[i]	X–H···Cg[j]	X···Cg[k]
C(91)–H(91) → Cg(6)	2.72	2.68	8.82	140	3.492

Potential H bonds				
D–H···A	H···A	Angle (deg) D–H···A	D–H	A···D
C(213)–H(21A)···O(11)d	2.57	146	0.99	3.4340(16)
C(213)–H(21B)···O(11)b	2.39	162	0.99	3.3446(17)
C(223)–H(22B)···O(11)d	2.53	147	0.98	3.3924(18)
C(233)–H(23A)···O(21)b	2.58	148	0.98	3.4513(17)
C(233)–H(23C)···O(11)d	2.51	148	0.98	3.3798(17)
C(243)–H(24B)···O(21)b	2.40	151	0.99	3.3027(16)
C(43)–H(43)···O(31)d	2.54	156	0.95	3.4268(16)

[a] Distance between ring centroids (Å). [b] Dihedral angle between planes I and J (°). [c] Angle between Cg(I) → Cg(J) vector and normal to plane J (°). [d] Angle between Cg(I) → Cg(J) vector and normal to plane I (°). [e] Perpendicular distance of Cg(I) on ring J. [f] Ring centroid Cg(5) of adjacent MO anion. [g] Distance between H(I) and ring centroid Cg(J) (Å). [h] Perpendicular distance of H(I) on ring J (Å). [i] Angle between H(I) → Cg(J) vector and normal to plane J (°). [j] Angle defined by X(I), H(I) and Cg(J) (°). [k] Distance between X(I) and Cg(I) (Å).

for [**9**]Br_8. This indicates that the host–guest properties can be fine-tuned by altering by the nature of the outer shell of the ionic core–shell dendrimers.

Discussion

The structural aspects and the host–guest binding properties of polyionic core–shell dendrimers have been studied by structurally investigating molecular components that represent defined structural sections of the dendrimers. Di- and mono-ionic dendritic wedges [**3**]Br_2 and [**4**]Br were successfully prepared and used as model compounds for ionic core–shell dendrimers [**1**]Br_8 and [**2**]Br_4 (Fig. 1), respectively. Alike the dendrimers, both wedges form discrete stoichiometric host–guest assemblies with Methyl Orange anions (MO) (Fig. 2). The experiments showed that the number of MO anions accommodated by the dendritic wedges is predefined by their number of ammonium groups. The diagnostic shifts

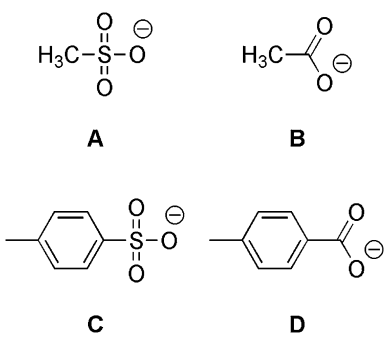

Fig. 9 Methyl sulfonate (**A**), acetate (**B**), *p*-toluenesulfonate (**C**) and *p*-methyl benzoate (**D**), which were used as anionic substrate molecules.

observed in the ^{1}H NMR spectra of [**3**]Br_2 and [**4**]Br upon formation of these MO assemblies indicate that the sulfonato group of MO is located nearby the ammonium site(s) of the wedges. The host–guest behavior displayed by the wedges towards MO guest molecules is similar to that of the ionic core–shell dendrimers, which justifies their use as model species for these dendrimers.

Structural aspects of [3]Br_2 and [4][MO]

Despite the extensive use of Fréchet-type poly(benzyl aryl ether) wedges in a wide variety of fields,[20] including host–guest chemistry, to date few X-ray crystal structures of Fréchet-type dendrons have been reported.[21] The X-ray crystal structure of [**3**]Br_2 contains two distinctive binding sites for the bromide anions (binding sites A and B in Fig. 4). In theory, similar binding sites could also be present in octaionic dendrimer [**1**]Br_8, which comprises four of these dendritic wedges around a silicon atom (Fig. 1). In that case, four bromide anions of ionic core–shell dendrimer [**1**]Br_8 would be embedded in the clefts of the four wedges, whereas the other four would be located in the internal voids between adjacent dendritic wedges. A schematic two-dimensional representation of this host–guest arrangement is actually depicted in Fig. 1. Tetra-

Table 6 Competition experiments with octa-ionic dendrimers [**1**]Br_8 and [**9**]Br_8, and wedges [**4**]Br and [**3**]Br_2 and *p*-toluenesulfonate (**C**), and *p*-toluenecarboxylate (**D**) guests in a biphasic water/dichloromethane set-up

Dendrimer	Exchanged anions (%)	Exchange ratio **C**/**D**
[**4**]Br	86	93
[**3**]Br_2	86	100
[**1**]Br_8	81	88
[**9**]Br_8	95	95

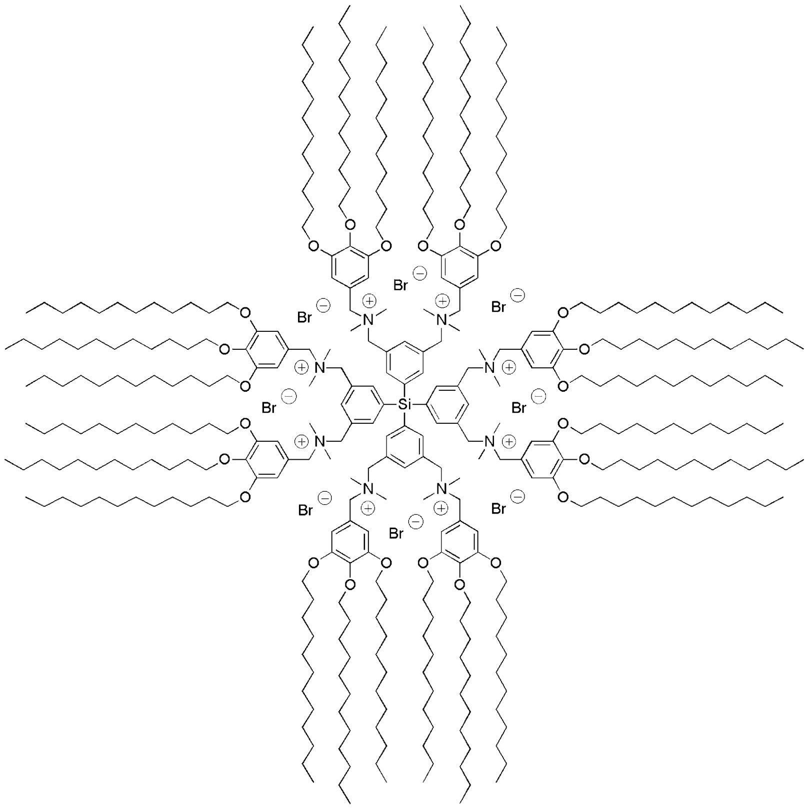

[**9**]Br_8

Fig. 10 Core–shell dendrimer [**9**]Br_8 with an apolar outer shell of 24 dodecyl groups.

ionic core–shell dendrimer [**2**]Br_4 (Fig. 1) is constructed from four mono-ionic dendritic wedges [**4**]Br around a silicon atom. On the basis of the structural aspects of mono-cationic wedge [**4**]$^+$ in the X-ray crystal structure of [**4**][MO], ionic core–shell dendrimer [**2**]Br_4 is expected to have only one type of binding sites for its four bromide anions.

The short distances between the bromide anions and several hydrogen atoms and the corresponding large C–H···Br angles point to weak hydrogen bonds between binding sites of di-cationic wedge [**3**]$^{2+}$ and the bromide anions. It should be mentioned, however, that the true nature of the short distances between hydrogens of a quaternary ammonium group is questioned in literature[16] since the short distances could also be solely due to the attracting Coulombic interactions between the cationic ammonium and the anion. The hydrogens, in this case, repulse the anion and prevent it from getting closer to the cationic site. In theory, a hydrogen bond is involved when the distance between hydrogen bond acceptor (A) and hydrogen bond donor (D) in A···H–D is shorter than the sum of the van der Waals' radii[22,23] of D and A increased with 0.50 Å. Furthermore, the distance between the hydrogen (H) and the hydrogen bond acceptor (A) is shorter than the sum of the van der Waals' radii of H and A reduced with 0.12 Å. Finally, the angle between D–H···A should exceed 100°. In the present case, a bromide atom can serve as hydrogen bond acceptor and a carbon atom as hydrogen bond donor. The distance between a bromide atom and a hydrogen atom should be less than 2.93 Å and the distance between a bromide atom and the carbon atom of a C–H hydrogen bond donating group should be shorter than 4.05 Å. The angle defined by the bromide, the hydrogen, and the carbon atom should exceed 100°. The distances between the bromide anions and hydrogen atoms of the binding sites A and B as well as the corresponding C–H···Br angles meet these requirements, and can therefore be considered as weak hydrogen bonds.

The relatively short distance between H(29) on ring (4) and the π-system of ring (6) as well as the arrangement of the C(29)–H(29) bond relative to phenyl ring (6) point to weak C–H···π interaction between these groups at the end of the wedge.[24]

Br(1) is positioned precisely above ring centroid Cg(1) of the phenyl ring (1) at the focal point of the dendritic wedge, which suggests non-covalent interactions between the bromide anion and the π-system of the aromatic ring. In contrast with cation–π interactions,[25] so-called anion–π interactions are not very common and only observed between lone-pair electrons of electronegative atoms, *e.g.* F, Cl, Br and O, and benzene rings with multiple strong electron-withdrawing substituents, such as C_6F_6.[26] In the reported systems, the angle defined by the interacting atom, the center of gravity of the ring (Cg), and one of the carbon atoms of the ring (C_{ring}) is close to 90°, whereas the average distance of all six X···C_{ring} is shorter than the sum of the van der Waals' radii, which is 3.62 Å in case of a Br···π interaction. In the present case, the angle defined by Br(1), Cg(1), and C(1) of the phenyl ring is close to 90°. The distance between Br(1) and Cg(1) (4.222(3) Å) is,

however, longer than the sum of van der Waals' radii. It is interesting to compare the properties of phenyl ring (1) in [**3**]Br_2 with the observations made for $Br\cdots\pi C_6F_6$ binding.[24] The difference in binding properties can be explained on the basis of the *m*olecular *e*lectronic *p*otential (MEP) of these molecules above the molecular plane. Calculations showed the presence of a positive region above the C_6F_6 plane due to the large number of electron withdrawing fluoro groups. The phenyl ring (1) of [**3**]Br_2, however, lacks multiple such electron withdrawing groups. It can be assumed that the region above the plane of ring (1) is less positive than that in the case of C_6F_6.[26] The anion–π interaction in the present host–guest complexes can, therefore, be expected to be relatively weak or even repulsive in nature, which implies that the binding of bromide anions by the wedge would be established mainly by Coulombic interactions and weak hydrogen-bonding.

The X-ray crystal structure MO assembly [**4**][MO] showed monocationic wedge $[\mathbf{4}]^+$ and the MO anion as a 1 : 1 host–guest assembly. The MO anion is directed with its sulfonato group towards the ammonium group of the wedge. This substrate positioning is in line with the results obtained by NMR spectroscopy. It is noteworthy that the oxygen atoms of the sulfonato group of MO are located further away from the ammonium site than the bromide anions in the crystal structure of [**3**]Br_2. It is interesting to compare the structure of [**4**][MO] with the structure reported for the sodium salt of MO.[27] The molecular geometry of the MO anion of [**4**][MO] is similar to the geometry found for Na[MO]. The crystal structure of Na[MO] showed layers of MO–MO dimers. The sulfonato groups in each dimer are mutually directed to opposite sites and are hydrogen bonded to a layers of co-crystallized water and ethanol molecules. The intra-atomic distances between the sulfur and the oxygen atoms of the sulfonato group are similar to the ones found in the crystal structure of [**4**][MO], *i.e. ca.* 1.45 Å. In analogy with Na[MO], the crystal lattice of [**4**][MO] also comprises discrete MO–MO dimers, which, however, are intercalated by dendritic wedges. In the case of Na[MO], the sodium cation and the solvent molecules are too small to effectively intercalate between the dimers of the MO–MO dimer layer. The edge-to-face arrangement of MO relative to a planar benzyl aryl ether moiety of the wedge points to π–π interactions between the MO anion and the dendritic wedge $[\mathbf{4}]^+$ (Fig. 7).[24]

The short distances between the oxygen atoms of the sulfonato group and hydrogen atoms of the ammonium CH_2 and CH_3 groups and aryl protons of dendritic wedge $[\mathbf{4}]^+$ point to hydrogen bonding interactions between the sulfonato group of MO and the dendritic wedge.[16,22,23] These findings are supported by the diagnostic shifts observed in the ^1H NMR spectra of [**4**]Br upon formation of MO assembly [**4**][MO]. Especially, the hydrogen atoms involved in hydrogen-bonding protons displayed significant shifts in the NMR spectra.

Substrate selectivity

The preliminary competition experiments with several substrate molecules in a biphasic system revealed that anionic substrates with a small aliphatic moiety, *i.e.* a methyl group, and a carboxylato or sulfonato group are not extracted from the water layer by ionic core–shell dendrimer [**1**]Br_8 and dendritic wedges [**3**]Br_2 and [**4**]Br. On the contrary, anionic substrate molecules with an aryl moiety, *i.e.* a *p*-tolyl group in combination with a sulfonato group, are readily accommodated by dendritic hosts in the dichloromethane layer.

The binding preference for the sulfonato over the carboxylato anion can be explained by taking the basicity and geometry of the anion and the nature of the solvent medium into account.[28] Consideration of the nature of the solvent medium in which the anion binding takes place is of great importance. In the substrate competition experiments, biphasic set-ups of water and dichloromethane were used. The hydrophobicity of the different substrate anions plays an important role and, in fact, can be a driving force for the transfer of anions between both phases. The sulfonato anion, which is less basic (and more hydrophobic) than the carboxylato anion, is expected to have a higher affinity for the apolar dichloromethane layer than the carboxylato anion. This effect can lead to preferential binding of sulfonato anions over carboxylato anions by the ionic core–shell dendrimers in the dichloromethane layer. In addition, the geometry of the substrate anion can also influence the binding strength and selectivity for certain substrates. In the case of the ionic core–shell dendrimers, the tetrahedral geometry of the ammonium groups seems more suited for hydrogen bonding with the tetrahedral geometry of the sulfonato anion than for the trigonal planar geometry of the carboxylato anion. This better complementary of the sulfonato anion may also contribute to the overall selectivity of the dendrimers.

Conclusions

The structural aspects and the host–guest binding properties of ionic core–shell dendrimers, [**1**]Br_8 and [**2**]Br_4 (Fig. 1), which bear a polycationic core and a neutral shell of Fréchet-type poly(benzyl aryl ether) dendrons, have been investigated by means of dendritic wedges [**3**]Br_2 and [**4**]Br, which resemble one of the four wedges of dendrimers [**1**]Br_8 and [**2**]Br_4, respectively. Alike the dendrimers, these dendritic wedges form discrete stoichiometric assemblies with Methyl Orange anions to afford [**3**][MO]$_2$ and [**4**][MO] (Fig. 2). The crystal structures of dendritic wedge [**3**]Br_2 and host–guest assembly [**4**][MO] have been reported. The X-ray crystal structures of [**4**][MO], revealed that the anionic sulfonato group of the MO guest molecule is located nearby the ammonium group of the dendritic wedge. The molecular structure of dendritic wedge [**3**]Br_2, which comprises two ammonium sites, revealed that this wedge, in fact, contains two different binding sites for the two bromide anions in the solid state (Fig. 4).

Key points of the crystal structures of compounds [**3**]Br_2 and [**4**][MO] are that they indicate that the binding of anionic guest molecules by the dendrimers is not solely based on Coulombic interactions but that additional binding interactions, such as weak hydrogen bonds, can be involved. Moreover, these X-ray structures substantiate earlier speculations in literature on the presence of π–π interactions between Fréchet-type poly(benzyl aryl ether) dendritic wedges and aromatic

substrate molecules.[3d,6,29] We believe that these additional weak interactions do not play a pivotal role in the binding of guest molecules, but can, however, influence the final position of the anionic guest molecule and induce structural rearrangements of the (flexible) dendritic host molecule in the presence of a guest molecule. The substrate selectivity of the ionic core–shell dendrimers for sulfonato anions over carboxylato anions, as was revealed in competition experiments, was attributed to additional binding interactions in terms of hydrogen bonding between the oxy anion group and π–π interactions or hydrophobic interactions with the organic moiety of the substrate molecule. In order to effectively use the ionic core–shell dendrimers as container molecules for substrate molecules, one should select or design substrate molecules bearing both a anionic groups that is capable of accepting multiple weak hydrogen bonds (*e.g.* a sulfonato, a sulfato or a phosphato group) and an organic moiety that can establish additional binding interactions, such as, hydrophobic interactions of π–π interactions, with the dendritic shell of the dendrimer.

Acknowledgements

R. J. M. K. G. acknowledges the National Research Scholl Combination Catalysis (NRSC-C) for financial support. M. L. and A. L. S. were supported by The Netherlands Foundation for Chemical Sciences (CW) with financial aid from The Netherlands Organization for Scientific Research (NWO).

References

1 For recent reviews on dendrimer host–guest system, see for example: (*a*) C. N. Moorefield and G. R. Newkome, *C. R. Chim.*, 2003, **6**, 715; (*b*) M. W. P. L. Baars and E. W. Meijer, *Top. Curr. Chem.*, 2000, **210**, 131.
2 (*a*) J. F. G. A. Jansen, E. M. M. de Brabander-van den Berg and E. W. Meijer, *Science*, 1994, **226**, 1226; (*b*) M. Maciejewski, *J. Macromol. Sci., Pure Appl. Chem.*, 1982, **17**, 689.
3 (*a*) T. Habicher, F. Diederich and V. Grammlich, *Helv. Chim. Acta*, 1999, **82**, 1066; (*b*) G. R. Newkome and L. A. Godínez, *Chem. Commun.*, 1998, 1821; (*c*) G. R. Newkome, C. N. Moorefield, G. R. Baker, A. L. Johnson and R. K. Behera, *Angew. Chem., Int. Ed. Engl.*, 1991, **30**, 1176; (*d*) C. J. Hawker, K. I. Wooley and J. M. J. Fréchet, *J. Chem. Soc., Perkin Trans. 1*, 1993, **21**, 1287.
4 For dendritic host molecules binding guest molecules using specific hydrogen bonds, see for example: (*a*) G. R. Newkome, B. D. Woosley, E. He, C. N. Moorefield, R. Güther, G. R. Baker, G. H. Escamilla, J. Merrill and H. Luftmann, *Chem. Commun.*, 1996, 2737; (*b*) S. C. Zimmerman, Y. Wang, P. Bharathi and J. S. Moore, *J. Am. Chem. Soc.*, 1998, **120**, 2172; (*c*) D. K. Smith, A. Zingg and F. Diederich, *Helv. Chim. Acta*, 1999, **82**, 1225; (*d*) U. Boas, A. J. Karlsson, B. F. W. De Waal and E. W. Meijer, *J. Org. Chem.*, 2001, **66**, 2136.
5 For dendritic host molecules binding guest molecules *via* electrostatic interactions, see for example: (*a*) C. Valério, E. Alonso, J. Ruiz, J.-C. Blais and D. Astruc, *Angew. Chem., Int. Ed.*, 1999, **38**, 1747; (*b*) J. F. Kukowska-Latallo, A. U. Bielinska, J. Johnson, R. Spindler, D. A. Tomalia and J. R. J. Baker, *Proc. Natl. Acad. Sci. U. S. A.*, 1996, **93**, 4897.
6 A. W. Kleij, R. van de Coevering, R. J. M. Klein Gebbink, A. M. Noordman, A. L. Spek and G. van Koten, *Chem.–Eur. J.*, 2001, **7**, 181.
7 Methyl Orange is the official name for the sodium salt of the $[O_3SC_6H_4N{=}NC_6H_4NMe_2]$ anion. For clarity, we use the notation MO to designate the $[O_3SC_6H_4N{=}NC_6H_4NMe_2]$ anion throughout the paper.
8 (*a*) R. van de Coevering, A. P. Alfers, J. D. Meeldijk, E. Martinez-Viviente, P. S. Pregosin, R. J. M. Klein Gebbink and G. van Koten, *J. Am. Chem. Soc.*, 2006, **128**, 12700; (*b*) R. van de Coevering, M. Kuil, R. J. M. Klein Gebbink and G. van Koten, *Chem. Commun.*, 2002, **15**, 1636.
9 C. J. Hawker and J. M. J. Fréchet, *J. Am. Chem. Soc.*, 1990, **112**, 7638.
10 P. Steenwinkel, S. L. James, D. Grove, N. Veldman, A. L. Spek and G. van Koten, *Chem.–Eur. J.*, 1996, **2**, 1440.
11 G. M. Sheldrick, *SHELXS-97*, Universität Göttingen, Göttingen, Germany, 1997.
12 A. Altomare, M. C. Burla, M. Camalli, G. L. Cascarano, C. Giacovazzo, A. Guagliardi, A. G. G. Moliterni, G. Polidori and R. Spagna, *J. Appl. Crystallogr.*, 1999, **32**, 115.
13 A. L. Spek, *J. Appl. Crystallogr.*, 2003, **36**, 7.
14 This is without contribution of the disordered solvent molecules.
15 Cg(I) is the official notation of the centroid of ring I. Throughout the paper, we use this notation to designate the ring I as well as the corresponding centroid of ring I.
16 G. R. Desiraju and T. Steiner, *The Weak H-bond in Structural Chemistry and Biology*, Oxford University Press Inc, New York, 1999, p. 252.
17 The numbering scheme of the molecular structure of [**4**][MO] is based on the fact that this assembly comprises two molecular fragments, *i.e.* $[MO]^-$ (fragment 1) and $[\mathbf{4}]^+$ (fragment 2). The atoms of each fragment are numbered consecutively, whereupon the fragment number was added at the end of each given atom number. Carbon atom 1 of $[\mathbf{4}]^+$ (fragment 2) is labeled with C12, for example.
18 For comparison, in water the MO anion is completely dimerized above 0.2×10^{-3} M and undergoes further aggregation above 1×10^{-3} M, see: K. L. Kendrick and W. R. Gilkerson, *J. Solution Chem.*, 1987, **16**, 257.
19 For the preparation of octa-ionic dendrimer [**9**]Br_8, see: R. van de Coevering, P. C. A. Bruijnincx, C. A. van Walree, R. J. M. Klein Gebbink and G. van Koten, *Eur. J. Org. Chem.*, DOI: 10.1002/ejoc200600727.
20 For a review on Fréchet-type dendrimers and their applications, see: S. M. Grayson and J. M. J. Fréchet, *Chem. Rev.*, 2001, **101**, 3819.
21 Selected examples: (*a*) B. Karakaya, W. Clausen, K. Gessler, W. Saenger and A.-D. Schlüter, *J. Am. Chem. Soc.*, 1997, **119**, 3296; (*b*) E. C. Constable, C. E. Housecroft, M. Neuburger, S. Schaffner and L. J. Scherer, *Dalton Trans.*, 2004, 2635; (*c*) L. Shen, M. Shi, F. Li, D. Zhang, X. Li, E. Shi, T. Yi, Y. Du and C. Huang, *Inorg. Chem.*, 2006, **45**, 6188; (*d*) V. J. Catalano and N. Parodi, *Inorg. Chem.*, 1997, **36**, 537.
22 For C–H···Acceptor interactions, see: (*a*) T. Steiner, *Crystallogr. Rev.*, 1996, **6**, 1; H-bond classification; (*b*) G. A. Jeffrey, H. Maluszynska and J. Mitra, *Int. J. Biol. Macromol.*, 1985, **7**, 336.
23 Default contact radii are those given in: A. Bondi, *J. Phys. Chem.*, 1964, **68**, 441. Contact radii (in Å): C, 1.70; H, 1.20; Br, 1.85; N, 1.55, O; 1.52. When the contact radii are not given one can use the sum of the covalent radius + 0.8 Å as critical distance.
24 (*a*) C. A. Hunter and J. K. M. Sanders, *J. Am. Chem. Soc.*, 1990, **112**, 5525; (*b*) G. B. McGaughey, M. Gagné and A. K. Rappé, *J. Biol. Chem.*, 1998, **273**, 15458.
25 J. C. Ma and D. A. Dougherty, *Chem. Rev.*, 1997, **97**, 1303.
26 (*a*) I. Alkorta, I. Rozas and J. Elguero, *J. Am. Chem. Soc.*, 2002, **124**, 8593; (*b*) D. Quiñonero, C. Garau, A. Frontera, P. Ballester, A. Costa and P. M. Deyà, *Chem. Phys. Lett.*, 2002, **359**, 486; (*c*) D. Quiñonero, C. Garau, C. Rotger, A. Frontera, P. Ballester, A. Costa and P. M. Deyà, *Angew. Chem., Int. Ed.*, 2002, **41**, 3389.
27 A. W. Hanson, *Acta Crystallogr., Sect. B*, 1973, **29**, 454.
28 For a reviews on anion recognition, see for example: (*a*) P. D. Beer and P. A. Gale, *Angew. Chem., Int. Ed.*, 2001, **40**, 486; (*b*) F. P. Schmidtchen and M. Berger, *Chem. Rev.*, 1997, **97**, 1609.
29 (*a*) J.-F. Nierengarten, L. Oswald, J.-F. Eckert and N. Armaroli, *Tetrahedron Lett.*, 1999, **40**, 5681; (*b*) M. Numata, A. Ikeda, C. Fukuhara and S. Shinkai, *Tetrahedron Lett.*, 1999, **40**, 6945.

